

Examining topographic effects from
earthquake-induced ground motions: Case study of
the Port Hills, New Zealand

Final Report for project EQC 15/U703

Brendon A. Bradley¹ and Seokho Jeong¹

¹Department of Civil and Natural Resources Engineering, University of
Canterbury, New Zealand

29 June 2017

1 Executive Summary

Many areas of New Zealand reside on topographically irregular terrain (i.e. hills, canyons), which influences the ground shaking felt in these areas. Currently, so-called topographic effects are not explicitly considered in conventional ground motion prediction, which results in greater modelling uncertainty. This report presents research over the past two years in order to enhance the holistic consideration of topographic effects in ground motion prediction through a combination of experimental data collection and 2D numerical analysis, through to the holistic consideration of topographic effects in 3D ground motion simulation methods. We summarise the technical capability developments in these areas through this small project, and with the international collaborations developed and on-going, where we expect this research to go in the near future.

Contents

- 1 Executive Summary** **2**

- 2 Technical Abstract** **4**

- 3 Motivation** **4**

- 4 Topographic amplification from recorded ambient vibration** **6**
 - 4.1 Experimental equipment and configuration 6
 - 4.2 H/V ratios of experimental observations 6
 - 4.3 Experimental spectral amplitudes 9

- 5 Two-dimensional numerical simulation** **10**
 - 5.1 Numerical model 10
 - 5.2 Spectral ratios from 2D numerical analysis 12

- 6 Three dimensional numerical simulation** **13**
 - 6.1 3D numerical model of the Port Hills 14

- 7 Discussion** **16**

- 8 Acknowledgements** **18**

2 Technical Abstract

This report provides a summary of research to enhance capability development for the explicit modelling of topographic effects in strong ground motion prediction. We consider observations for the 2010-2011 Canterbury earthquakes, as well as undertake ambient vibration field testing to obtain data used to understand topographic amplification in the Christchurch Port Hills. We then perform 2D simulations to corroborate the field testing observations, and then finally generalise to the consideration of topographic effects in 3D ground motion simulations. Through collaborations developed with international research teams we provide a forward look toward developments that we expect to happen in the near future in order to consider this important phenomena in strong ground motion prediction.

3 Motivation

Both historical and recent earthquakes have provided notable anecdotal evidence for the importance of surface topography on the localised amplification of earthquake-induced ground motions [Ashford et al., 1997]. For example, the damage patterns in the Port Hills, Christchurch, NZ, shown in Figure 1, suggest strongly amplified ground motions relative to those observed on the flat alluvial plains of Canterbury. Such ground motion amplification, and the consequences in terms of damage to structures and ground destabilization (e.g. rockfalls and slope instability) are significant. Recently, the NZ government further red zoned houses in the Canterbury region which were deemed to be at excessive ongoing hazard. Despite the observed issues in the Port Hills during the Canterbury earthquakes, the impact of topographic effects and their associated consequences will be likely greater in future earthquakes in the Wellington region, for example, where a significantly greater portion of the urban area occurs in topographically irregular terrain. Despite evidence from past earthquakes, the current conceptual models of topographic effects provide limited predictive capabilities because of their highly simplified assumptions. As a result, topographic amplifications remain poorly understood, and the effect of

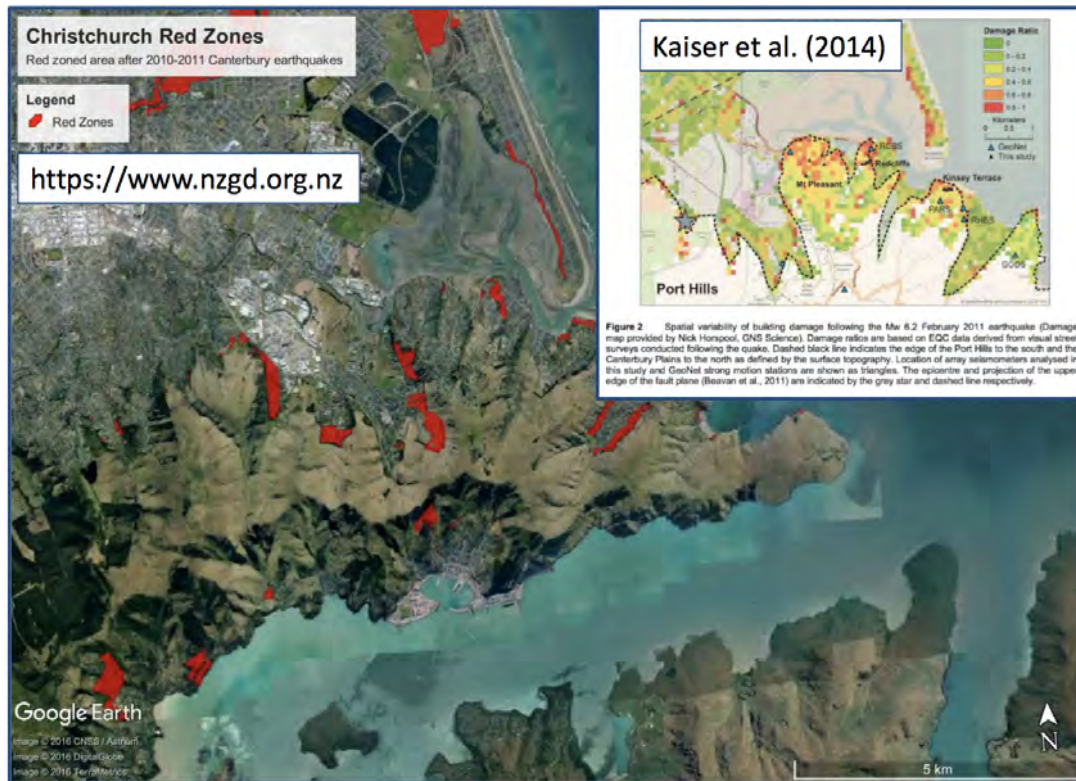


Figure 1: Damage observations in the Port Hills area of Christchurch during the Canterbury earthquake sequence [Kaiser et al., 2014].

topographic amplification is completely absent from NZ design codes [NZS 1170.5, 2004] (as well as all others worldwide with only two exceptions).

In order to better understand topographic effects, and develop predictive models, a direct incorporation of the real-world complexity is needed. This complexity exists both in terms of the irregular topography and also the spatial variation of subsurface soil conditions. Naturally, incorporating such complexity on a regional scale can substantially increase computational demands beyond the point of simple workstation-based modelling capabilities. This has therefore resulted to date in the use of highly simplified models, and as a result, poor predictive capabilities [Ashford et al., 1997].

This research project aims to initialise capability developments for the explicit modelling of topographic effects in strong ground motion prediction. We consider observations for the 2010-2011 Canterbury earthquakes [Bradley, 2016, Kaiser et al., 2014], as well as undertake ambient vibration field testing to obtain data used to understand topographic amplification in the Port Hills. We then perform 2D simulations to corroborate the field testing observations, and then finally generalise to the consideration of 3D simulations.

Through collaborations developed with international research teams we provide a forward look toward developments that we expect to happen in the near future in order to consider this important phenomena in strong ground motion prediction.

4 Topographic amplification from recorded ambient vibration

4.1 Experimental equipment and configuration

Past studies have shown that the effect of topography on the observed ground motions can be observed, not only during the earthquakes, but also under the ambient condition [Stolte et al., 2017]. We deployed eight portable seismometers (Trillium compact 20s by Nanometrics) for the duration of two months (March-April 2017) along a linear array in Mount Pleasant and Heathcote Valley as shown in Figure 2, to investigate the role of surface topography on the characteristics of recorded ambient vibrations. Figure 3 shows a photo of a seismometer (S06) deployed in Heathcote Valley.

The measured ambient vibration records were divided into multiple time windows that have a duration of 120s. Each time window was then tapered using the Tukey (tapered cosine) window with a tapering duration of 5% (i.e. the first 2.5% and the last 2.5% of the windowing function equals to parts of a cosine). The Fourier amplitude spectrum for each tapered time window is then smoothed using the Konno-Ohmachi smoothing window with the bandwidth constant $b = 40$. Subsequently, the single-station horizontal-to-vertical spectral ratios (HVSr) and the standard spectral ratios (SSR) are computed using the smoothed Fourier amplitude spectra.

4.2 H/V ratios of experimental observations

Figure 4 illustrates the horizontal-to-vertical spectral ratios obtained through the analysis of the ambient vibrations at the individual sensors shown in Figure 2. On the basis that near-surface site response has a limited effect on vertical vibrations, the H/V ratio is



Figure 2: Location of experimental transect in Heathcote Valley / Mt Pleasant, indicating sensor locations and topographic profile.



Figure 3: An example of the portable seismometer deployment.

often used to infer the modal frequencies of site response as a result of stratigraphic and/or topographic effects.

For example, the stations within the valley (S08, S07, S06, and S04) show peaks with high amplitudes at different predominant frequencies, gradually increasing from $f_0 =$

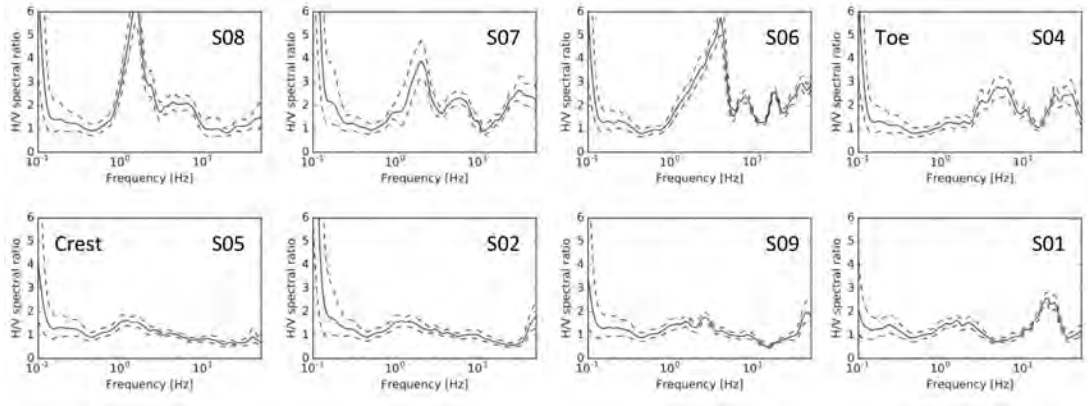


Figure 4: Observed horizontal-to-vertical (H/V) spectral ratios from ambient vibrations $1.5Hz$ at S08 to $f_0 = 6Hz$ at S04, as the station gets closer to the basin edge. It is expected that the sharp impedance contrast at the soil-bedrock interface is primarily responsible for such high amplification within the valley, while it is well known that the three-dimensional basin geometry may further modify the characteristics of the surface ground motions.

On the other hand, the stations on the hill (S05, S02, S09, and S01) show a relatively flat curve in the H/V ratio plots, which reflects the fact that those sites are situated on a very thin layer of surficial soil overlying the Port Hills volcanic rock. For example, at S05 near the crest, the rock outcrops are visible and the H/V ratio does not show any noticeable peak up to $f = 50Hz$, whereas the high frequency peaks visible in S01 (and partly visible in S02 and S09) may be attributed to the response of the shallow surficial soil.

Interestingly, all stations situated on the hill (S05, S02, S09, and S01) consistently exhibits a slight bump near $f = 1.5Hz$. While it is not possible to identify the source of such response by the H/V spectral ratios alone, the frequency is consistent with the “topographic frequency” proposed by Ashford et al. [1997]:

$$f_0^{Topo} = \frac{V_S}{5h} = \frac{1500m/s}{5 \times 200m} = 1.5Hz \quad (1)$$

4.3 Experimental spectral amplitudes

The Fourier spectra of recorded ambient vibrations can be normalised by the spectrum from a reference station to demonstrate the effect of surface topography. Ideally, the reference free-field station would have a flat topography and satisfy the “free-field condition”, meaning that it would be free from the scattered wavefield. At the same time, the reference station needs to have similar geology and similar bedrock motions with the rest of the stations, which requires some proximity with the rest of the stations. Obviously, satisfying all these conditions simultaneously is extremely challenging, and a compromise is often required when choosing a reference site. For this study, we chose S04 at the toe as the reference station. The recorded motions at this station would be affected by the response of shallow soil, but it is expected to be limited in the high frequency only, as it was confirmed in Figure 4. We acknowledge that the ground motions are deamplified at the toe of the slope, and therefore the topographic spectral ratios could be overestimated, if the Fourier spectra of all stations are free of the near surface soil effect near the topographic frequency.

Figure 5 shows the standard spectral ratios with S04 as reference. The ground motions at stations on the Hill (S05, S02, S09, and S01) are consistently amplified at $f_0 = 1.5Hz$, which is consistent with the observation made from the H/V spectral ratios. The highest amplification occurs at stations near the crest (S05 and S02), and the amplification factor is approximately 1.7 for the N-S component and 1.3 for the E-W component at those stations, whereas the amplification factor gradually decreases as the stations get farther away from the crest.

A direct consequence of using S04 as a reference station is the apparent deamplification at frequencies $f > 3Hz$ of the stations on the hill, which is most likely caused by the flat responses of hill stations being normalized by the high frequency amplification of S04. Also, all the stations within the valley have large spectral ratios in frequencies $f > 1Hz$, which demonstrates the dynamic response of the shallow soil on the recorded ambient vibrations.

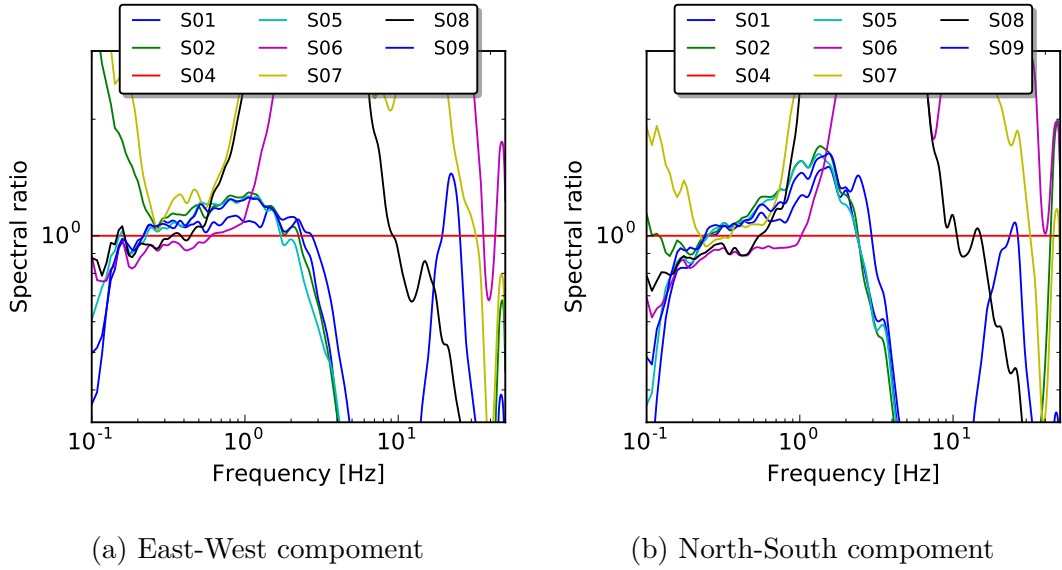


Figure 5: Ambient vibration spectral amplitudes for: (a) Horizontal East-West; (b) Horizontal North-South directions relative to the vibration amplitude at the toe of the slope (S04).

5 Two-dimensional numerical simulation

5.1 Numerical model

In order to examine the salient topographic features present in the experimental observations, 2D numerical analyses were undertaken. Figure 6 illustrates the finite element mesh that was generated using the software GMSH and subsequently used in SpecFem2D software to perform the 2D numerical simulations. Because focus was on the modelling of topographic effects, the material properties of the model were homogeneous with a shear wave velocity of $V_s=1500\text{m/s}$ (as part of work on-going beyond the deadline of this project are more detailed analysis is being performed as elaborated upon in the discussion section).

Figure 7 illustrates the effects of surface topography via a plot of simulated waveforms as a function of time and offset location (i.e. along the length of the model). The simulation uses a $f=12\text{Hz}$ Ricker wavelet as input motion in order to emphasise the effect of the geometric features on the resulting surface ground motions (and not the effect of a complex earthquake-induced ground motion, for example). It can be seen in the figure that there is constructive interference at the crest of the slope.

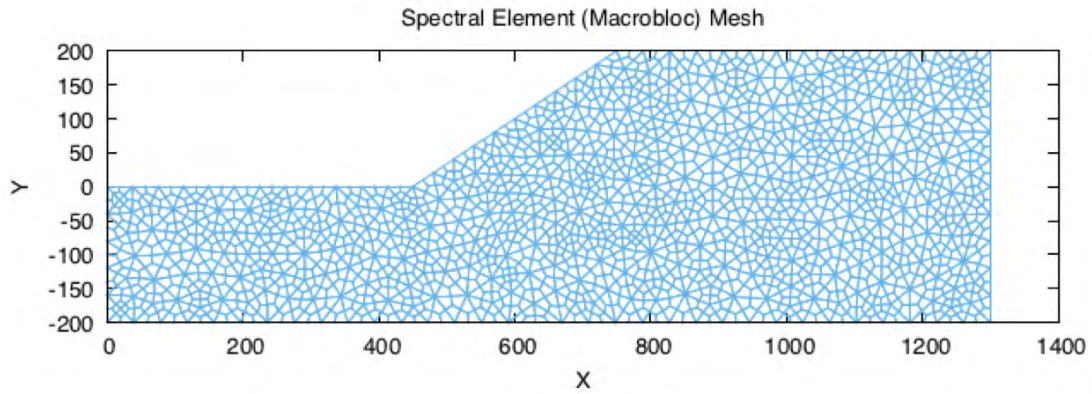


Figure 6: Finite element mesh of 2D numerical simulation used to examine topographic effects in the context of the experimental ambient vibration array deployed in Figure 2. X and Y dimension are in metres.

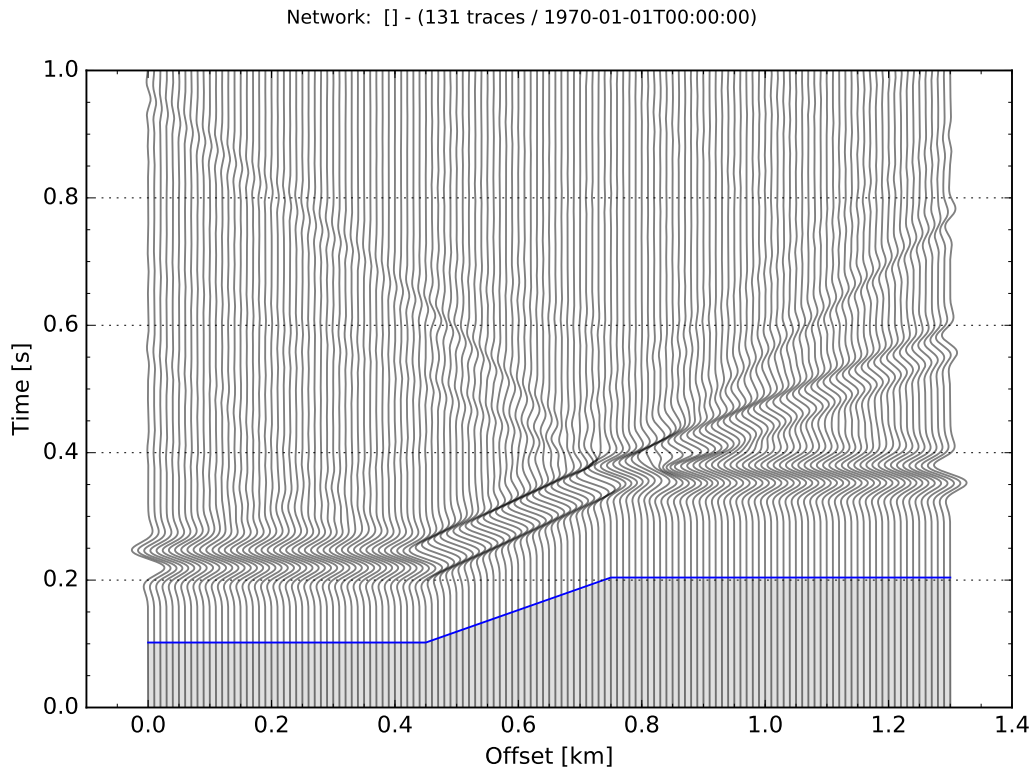


Figure 7: Illustration of simulated waveforms at the surface of the model as a function of linear offset (i.e. location along the slope) and time. The constructive and destructive interference patterns that results from the irregular free surface due to topography can be seen.

Figure 8 provides a summary of the topographic amplification from the simulation in the form of the ratio of peak ground velocity as measured along the surface divided by that in the free-field (i.e. to the left and right hand extents of the model, where the effects of the slope topography are negligible). There are two significant features evident

in Figure 8, firstly, the large amplification that occurs at the crest of the slope as a result of constructive interference (with PGV/PGV_{ff} ratios of approximately 1.8); and secondly, appreciable deamplification at the toe of the slope where the ratio is approximately 0.8. It is also noted that along the length of the inclined slope the ratio is generally slightly less than 1.0, and on top of the slope near the crest there is a large variation in the ratio as a function of the distance from the slope crest.

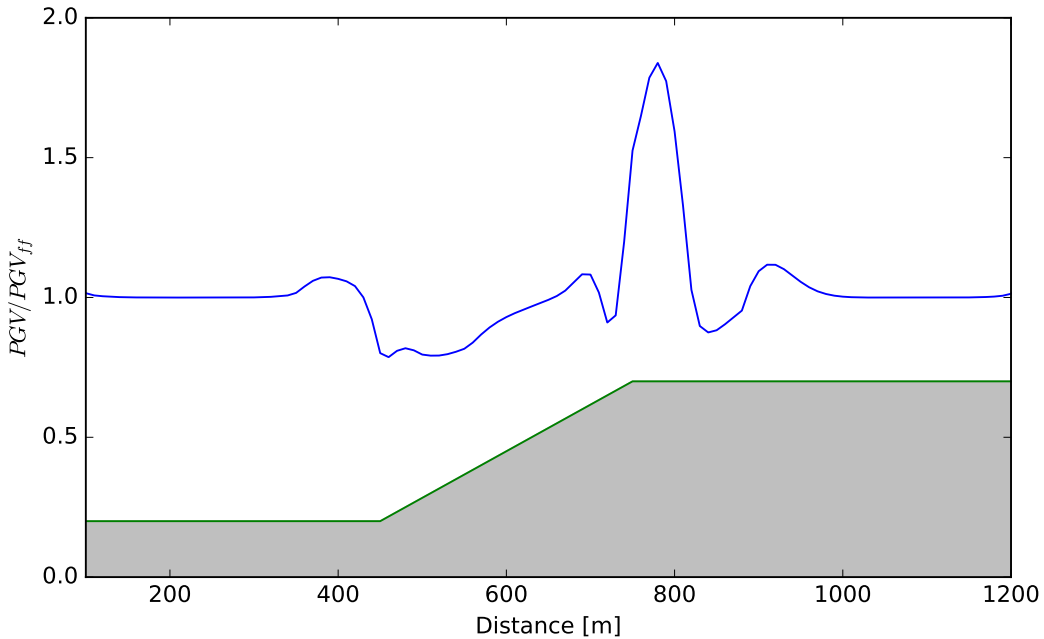


Figure 8: Ratio of peak ground velocity along the model surface (PGV) divided by the free-field peak ground velocity (PGV_{ff}) illustrating the effects of surface topography.

5.2 Spectral ratios from 2D numerical analysis

To compare the 2D numerical simulation with the measured ambient vibrations, we recorded the simulated motions at the equivalent locations as the field experiment. Figure 9 illustrate the standard spectral ratios from the 2D simulation, with the station S04 at the toe as reference. The naming of the stations shown in Figure 9 is also consistent with Figure 5.

As our model assumes a homogeneous $V_S = 1500m/s$, the computed spectral ratios do not exhibit the amplifications caused by the soil-bedrock velocity contrast that was present in the observed spectral ratios. Rather, the spectral ratios shown in Figure 9 only

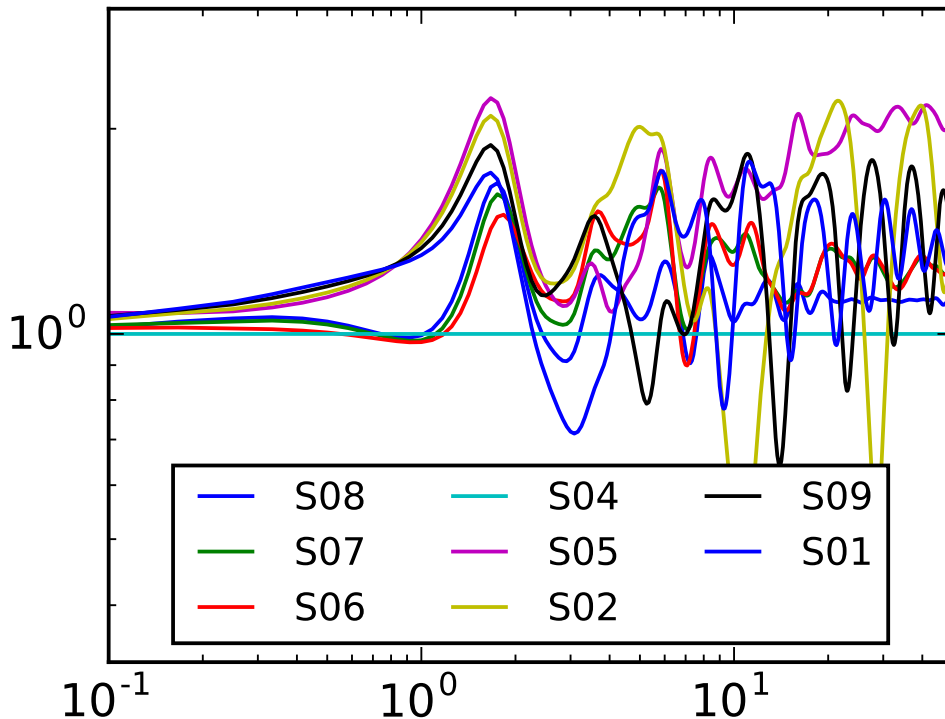


Figure 9: Horizontal spectral ratios from the 2D numerical simulation with S04 as reference. The locations and the naming of the stations are consistent with the field experiment.

describes the pure effect of surface topography, as all the considered stations have the identical velocity profile.

Albeit with some slight difference in the amplitudes, the simulated spectral ratios demonstrate the topographic amplification at $f = 1.5Hz$ that is consistent with our field experiment and the previous study by Ashford and Sitar (1997), which also suggests that the mild peaks observed in that frequency from the H/V spectral ratios may also be attributed to the effect of surface topography.

6 Three dimensional numerical simulation

We argue that the inconsistencies between theoretical topographic effects and empirical observations of topographic effects in either past earthquakes, or from ambient vibrations, are the result of the simplicity of prior theoretical considerations of topographic effects. In particular, this is generally the result of the consideration of simplified and 2D topog-

raphy with a single in-plane or out-of-plane excitation. Hence, we believe that greater consistency can be obtained by embracing the inherent complexity in this problem by explicitly modelling the complex 3D variation in the elevation of the earth’s surface¹.

Given the above philosophy we sought to use earthquakes and observations in the Canterbury earthquake sequence to explicitly consider topography in the free-surface of 3D simulations. In order to examine both validation of simulations against observational data, as well as verification of simulation computational algorithms and codes, we decided to adopt two different computational tools to numerically simulate 3D wave propagation - SpecFem3D and Hercules.

The first simulation code, the results of which are elaborated upon in detail here, make use of SpecFem3D (specifically, SpecFem3DCartesian), which uses a 3D spectral element formulation to explicitly represent non-planar surface topography. The second simulation code, which is being utilized in collaboration with researchers at the University of Memphis, is Hercules, which is an octree-based finite element code. Because of the octree-based nature of Hercules (which requires cubic 3D elements of fractal dimensions) then a ‘virtual topography’ approach is implemented to approximate the non-planar free surface. Further discussion on the collaboration with the University of Memphis is presented in the discussion section.

6.1 3D numerical model of the Port Hills

A 3D model of the computational domain considered in the SpecFem3D simulations is shown in Figure 10.

The surface topography and the bathymetry was represented by a global relief model ‘SRTM15_PLUS’ (topex.ucsd.edu/WWW_html/srtm30_plus.html), and the 3D meshing was performed automatically using the mesh generation software Trelis.

The grid spacing for the computational model is $\Delta x = 125m$ on the ground surface, and $\Delta x = 375m$ where the depth is greater than $1km$. The numerical simulations were performed on the ‘Pan’ high-performance computer at the University of Auckland which

¹explicit representation of complex near-surface stratigraphy is also important, as demonstrated by others, but in this report we focus principally on the effects of surface topography

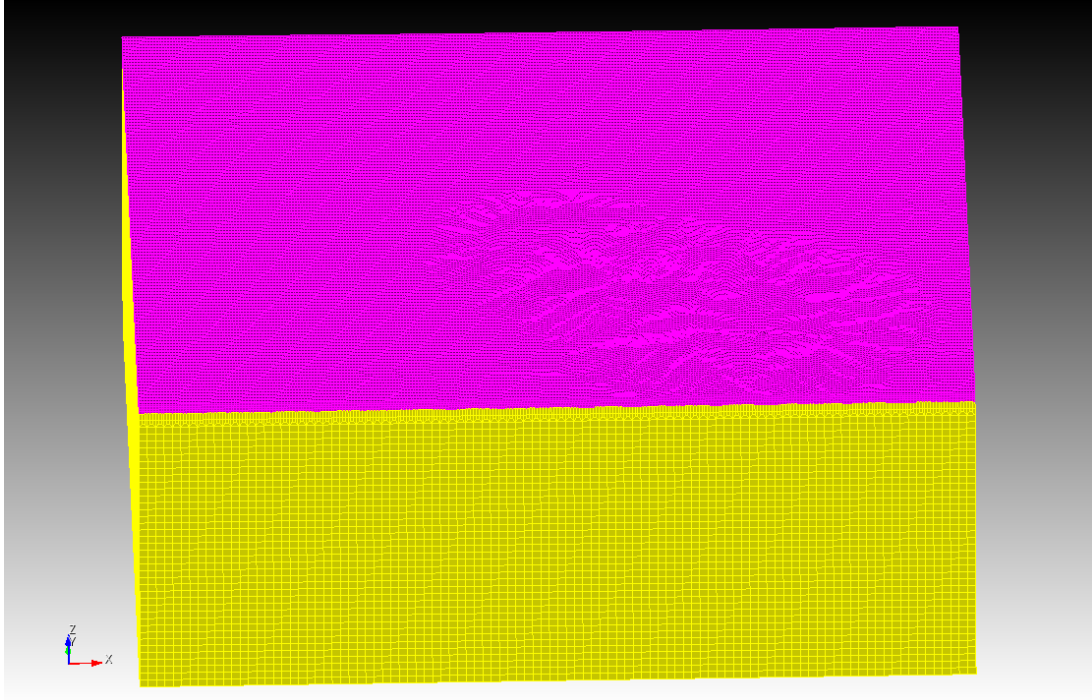


Figure 10: 3D computational mesh used in SpecFem3D, the topography of the Port Hills is evident in the near-surface.

is operated under NeSI. Each simulation was performed for the ground motion duration of 60 seconds, which takes approximately 10-20 hours to complete using 256 computer cores.

For the purposes of this report, we present preliminary results of 3D ground motion simulations for the M_W 6.0 13 June 2011 Christchurch earthquake, approximated as a point source using the seismic moment tensor solution from GeoNet. Figure 11 provides an illustration of the surface ground motion amplitudes (red and blue colors indicating positive and negative amplitudes). In Figure 11a the radiation pattern is evident, and then the scattering of the wave field as a result of the non-planar free-surface topography becomes evident in the subsequent time snapshots.

Figure 12 illustrates the simulated peak ground velocities at the ground surface with and without the consideration of topography. Figure 13 illustrates the logarithmic ratio of the PGV results shown in Figure 12 specifically focusing on the region around the Port Hills of Christchurch. Contours of zero indicate nominally equal simulated PGV values for with and without topography, positive values that the consideration of topography increases PGV, and negative values that it decreases the PGV.

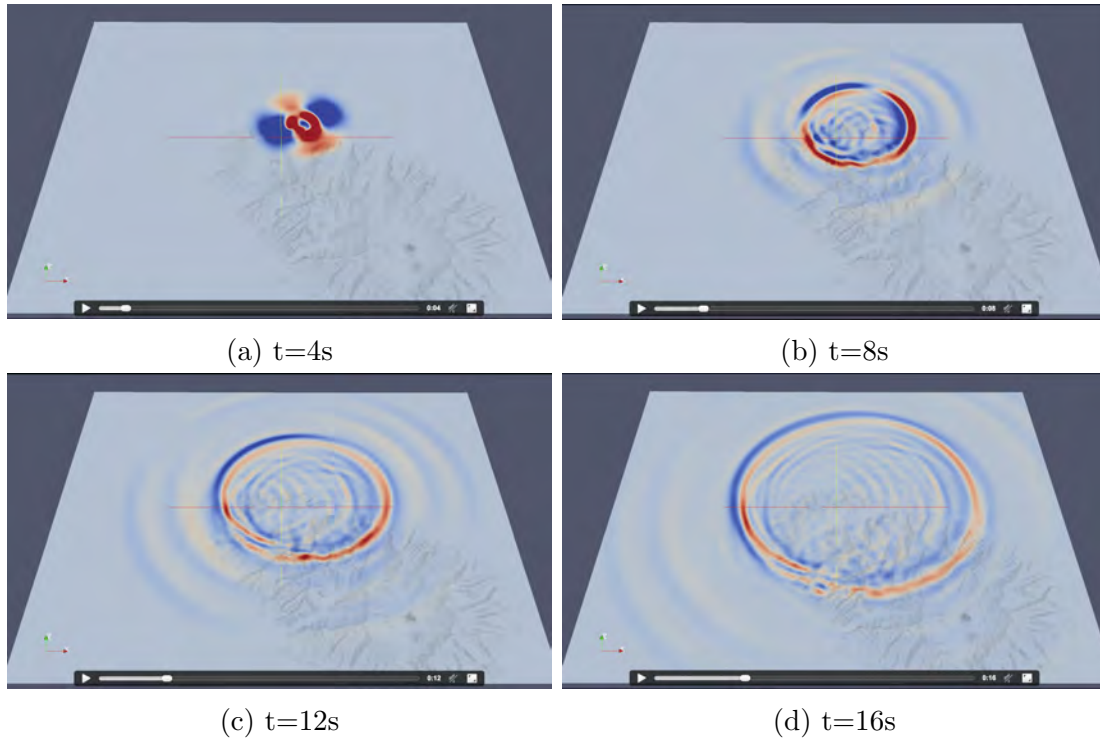


Figure 11: Illustration of 3D numerical simulation amplitudes at the ground surface for four time instants. The radiation pattern of the source is evident in the initial surface amplitudes, and the effect of topographic scattering is seen in the later time steps.

It can be seen that the pattern of this 'topographic amplification' is highly variable over the simulation region as a result of the topographic complexity of the earth's surface, which is modelled in detail using the digital elevation model. In general, topographic amplification occurs on hill crests, along hill ridges, and deamplification occurs at the base of the hills and in broader depressions.

However, these are general trends only, and the specifics are a function of the geometry and aspect ratio of the topographic features, and the frequency content of the ground motion.

7 Discussion

This report summarises the current status of our ongoing research effort for characterising the effect of surface topography on the earthquake ground motions, focusing on the observations made during the 2010-2011 Canterbury earthquakes.

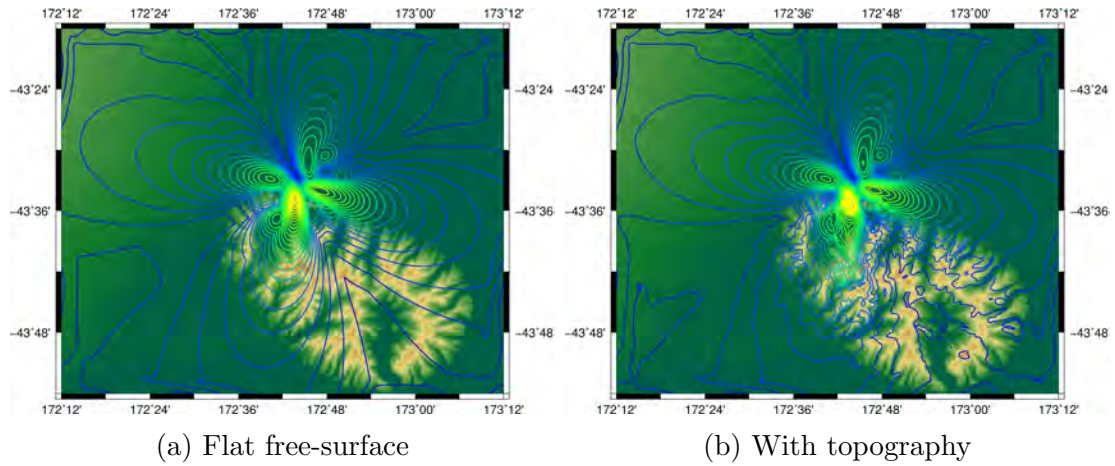


Figure 12: Comparison of the peak ground acceleration over the simulation domain for: (a) a flat free surface (no topography); and (b) considering topography.

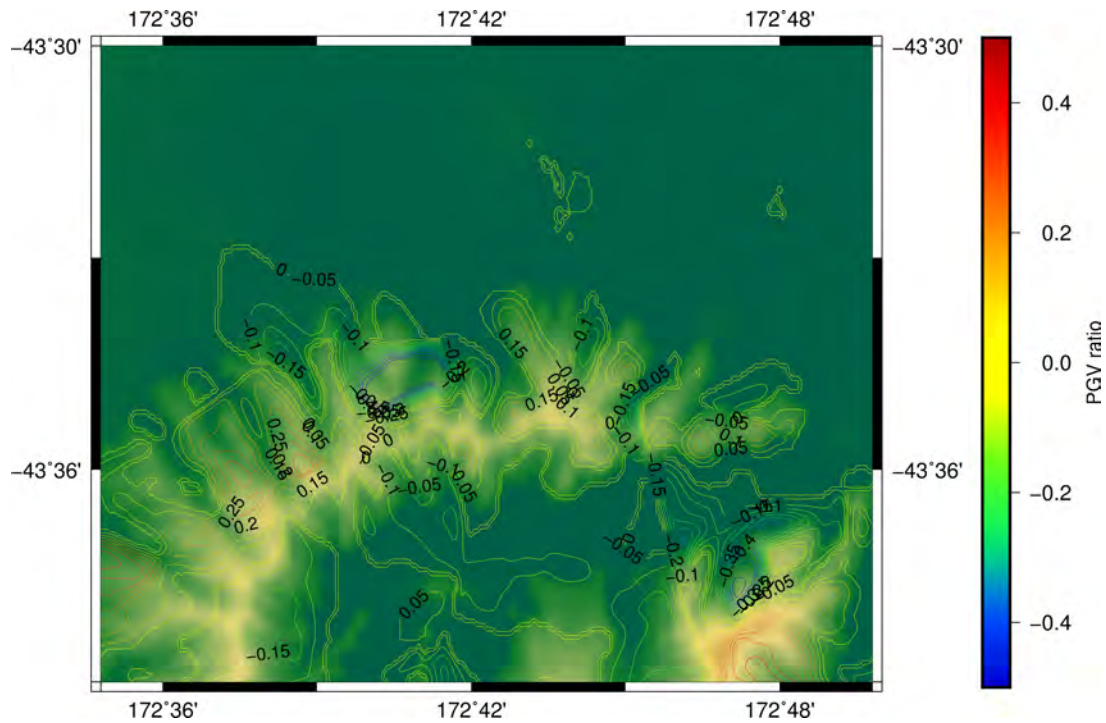


Figure 13: Logarithmic ratio of peak ground velocities simulated with and without topography.

We have shown that our field experiment and the 2D simulations consistently predicts the topographic amplification at $f = 1.5Hz$ near the crest of the slope in Mount Pleasant, Christchurch. However, the 2D simulation presented in this report shows only the preliminary results, assuming a simple homogeneous material with a synthetic earthquake. More realistic and detailed numerical analyses, to investigate the role of realistic velocity structure, is currently being lead by researchers at the California Institute of Technology

as a collaborative effort.

The 3D numerical simulations are yet to be validated using the recorded earthquake ground motions and the observed damage pattern in Port Hills. To achieve that, we recently started implementing the recently developed Canterbury Velocity model [Lee et al., 2017], and the finite fault models of the 2010-2011 Canterbury earthquakes within the Specfem3D workflow.

As previously discussed, a group of researchers at the University of Memphis are also investigating the effect of surface topography of Port Hills on the observed ground motions, using a computer program Hercules. Currently, they finished porting the code to the NeSI supercomputer ‘Fitzroy’, and implemented the Canterbury velocity model within the Hercules workflow. Their results will be compared with our results from Specfem3D, and the effects of model assumptions and different ways of formulations and implementations will be investigated.

8 Acknowledgements

The support of EQC in this capability development is greatly appreciated. This project was also partially supported from a Royal Society of New Zealand Rutherford Discovery Fellowship.

References

- Scott A. Ashford, Nicholas Sitar, John Lysmer, and Nan Deng. Topographic effects on the seismic response of steep slopes. *Bulletin of the Seismological Society of America*, 87(3): 701, June 1997. URL bssaonline.org/content/87/3/701.abstract.
- Brendon A. Bradley. Strong ground motion characteristics observed in the 13 June 2011 Mw6.0 Christchurch, New Zealand earthquake. *ICEGE ? Earthquake Geotechnical Engineering*, 91:23–38, December 2016. ISSN 0267-7261. doi: 10.1016/j.soildyn.2016.09.006. URL sciencedirect.com/science/article/pii/S0267726116302305.

A. Kaiser, C. Holden, and C. Massey. Site amplification, polarity and topographic effects in the Port Hills during the Canterbury earthquake sequence. Technical report, 2014. GNS Science Consultancy Report 2014/121.

R.L. Lee, B.A. Bradley, F. Ghisetti, and E.M. Thomson. Development of a 3d velocity model for the Canterbury, New Zealand region for broadband ground motion simulation. *Bulletin of the Seismological Society of America (accepted for publication)*, 2017.

NZS 1170.5. Structural design actions, Part 5: Earthquake actions - New Zealand. Technical report, Standards New Zealand, Wellington, New Zealand, 2004.

Andrew C. Stolte, Brady R. Cox, and Richard C. Lee. An Experimental Topographic Amplification Study at Los Alamos National Laboratory Using Ambient Vibrations. *Bulletin of the Seismological Society of America*, March 2017. doi: 10.1785/0120160269. URL bssaonline.org/content/early/2017/03/09/0120160269.abstract.